

15-A

T 73-14252

C.I

CR-128962

SPACE SHUTTLE GN & C EQUATION DOCUMENT

No. 22

APPROACH GUIDANCE

by

Yee-Chee Tao

N73-25707

(NASA-CR-128962) SPACE SHUTTLE GN AND C
EQUATION DOCUMENT NO. 22: APPROACH
GUIDANCE (Massachusetts Inst. of Tech.)

CSCS 17G

Unclas

G3/21 06247

31 p HC \$3.25

30

LIBRARY COPY

JUN 18 1973

JOHNSON SPACE CENTER
HOUSTON, TEXAS

CHARLES STARK DRAPER
LABORATORY

MASSACHUSETTS INSTITUTE OF TECHNOLOGY

CAMBRIDGE, MASSACHUSETTS, 02139

SPACE SHUTTLE GN & C EQUATION DOCUMENT

No. 22

Approach Guidance

by

Yee-Chee Tao

M. I. T. Charles Stark Draper Laboratory

December 1972

NAS9-10268

for

National Aeronautics and Space Administration

Systems Analysis Branch

Guidance and Control Division

Manned Spacecraft Center, Houston, Texas

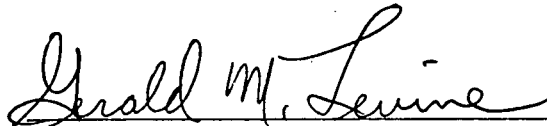
ACKNOWLEDGEMENT

This report was prepared under DSR Project 55-40800, sponsored by the Manned Spacecraft Center of the National Aeronautics and Space Administration through Contract NAS9-10268.

The publication of this report does not constitute approval by the National Aeronautics and Space Administration of the findings or the conclusions contained therein. It is published only for the exchange and stimulation of ideas.

FOREWORD

This document is one of a series of candidates for inclusion in a future revision of MSC-04217, "Space Shuttle Guidance, Navigation and Control Design Equations." The enclosed has been prepared under NAS9-10268, Task No. 15-A, "GN & C Flight Equation Specification Support", and applies to function 1 of the Approach Guidance Module (OG6), as defined in MSC-03690, Rev. C, "Space Shuttle Orbiter Guidance, Navigation and Control Software Functional Requirements - Vertical Flight Operations", dated 31 July 1972.

A handwritten signature in cursive script that reads "Gerald M. Levine". The signature is written in dark ink and is positioned above a horizontal line.

Gerald M. Levine, Director
APOLLO Space Guidance Analysis Division

TABLE OF CONTENTS

Section 1	Introduction
Section 2	Functional Flow Diagrams
Section 3	Input and Output Variables
Section 4	Description of Equations
Section 5	Detailed Flow Diagrams

NOMENCLATURE

Notational Conventions

Upper-case letters represent matrices

Lower-case and Greek letters reserved for scalars and vectors

Vector quantities are underlined, e. g. \underline{x}

Vectors are assumed to be column vectors unless explicitly noted

Symbols

a	Effective aerodynamic area of vehicle
\underline{a}	Acceleration (RW coordinate)
c_l	Coefficient of lift
c_{l_α}	$\partial(c_l) / \partial(\alpha)$
d_c	Rudder-flare command
d_{RT}	Distance between touchdown point and ED center
f_{turn}	Turning factor
g	Gravity
h	Altitude
\dot{h}	dh/dt
\ddot{h}	$d\dot{h}/dt$
h_1	Altitude at beginning of Initial Approach
h_R	Reference altitude
\dot{h}_R	$d(h_R)/dt$

k_1	Control gain
k_2	Control gain
k_{11}	Left or right HA selector
l_D	Desired lift specific force
m	Vehicle mass
m_v	Mach no.
M_{R-NED}	Run-way to NED Coordinate Transformation Matrix
q	Dynamic pressure
q_{old}	Dynamic pressure at last guidance call
q_D	Desired dynamic pressure
\dot{q}	dq / dt
q_v	$\partial q / \partial v$
rad	Radians into degree
r_{DME}	Distance from vehicle to Tacan
r_{ED}	Radius of ED cylinder
\underline{r}_{NED}	Horizontal component of vehicle position vector (NED-Tacan Coord.)
\underline{r}_{RT}	Horizontal component of position vector (RN-Tacan coord.)
s_{HE}	Integration of steady state heading error in Mode 2
s_m	Mode selector
t_c	Clock time

Δt	Time interval between guidance updates
\underline{u}_1	Unit vector (1, 0, 0)
\underline{u}_2	Unit vector (0, 1, 0)
\underline{u}_3	Unit vector (0, 0, 1)
\underline{v}	Vehicle velocity w. r. t. air mass
$\underline{v}_{\text{NED}}$	Horizontal component of vehicle velocity (NED Coord.)
\underline{v}_R	Vehicle velocity vector (R. W. Coord.)
$\underline{v}_{\text{RT}}$	Horizontal component of vehicle velocity (R. W. - Tacan Coord.)
y	Cross range to runway
\dot{y}	dy/dt
α	Current angle-of-attack
α_c	Angle-of-attack command
ϕ	Roll angle command magnitude
ϕ_c	Roll angle command
$\Delta\alpha_D$	Desired angle-of-attack change
$\Delta\psi_C$	Desired azimuth change
ψ	Azimuth ($0 \sim 360^\circ$)
ψ_c	Azimuth command ($0 \sim 360^\circ$)
ψ_{RW}	Runway azimuth
θ_{HA}	Azimuth of ($-\underline{\rho}_{\text{HAR}}$) vector

θ_N	Angle to Tacan w. r. t. north (from vehicle) (0 - 360°)
θ_T	Angle to Tacan w. r. t. velocity (from vehicle) (0 - 180°)
ρ	Air density
ρ_P	Predicted range to go to key point
$\underline{\rho}_{HAN}$	Vector from proper HA to vehicle (NED Coord.)
$\underline{\rho}_{HAR}$	Vector from proper HA to vehicle (RW-Tacan Coord.)
$\underline{\rho}'_{HAR}$	Vector from other HA to vehicle (RW-Tacan Coord.)
$\underline{\rho}_R$	Vehicle position vector in (RW Coord.)
ρ_{RD}	Distance to touchdown point
$\underline{\rho}_{HAT}$	Vector from Tacan to proper HA center (RW-Tacan Coord.)

Coordinates:

(RW Coord.)

Runway coordinates, centered at touchdown point

z in runway landing direction, i. e. directed down-range and forward
 x up
 y x, y, z from right hand orthogonal
 coordinates

(RW - Tacan Coord.)

Runway coordinates, centered at Tacan or center of EDC

(NED Coord.)

Local North, East, down coordinates at point of Tacan

Angle Measurements

(0, 360°) or (0 ≤ θ < 360°)

θ between 0 and 360°, measured clockwise

(0, 180°) or (-180° < θ ≤ 180°)

θ between (0 180°) if measured (clockwise)

(0 -180°) if measured (counter clockwise)

1. INTRODUCTION

The Approach Guidance Routine presented here is designed to take the orbiter vehicle from the end of the entry phase (altitude $\approx 100,000$ ft) down to the start of the terminal guidance phase 5.9 n. mi. from the runway at an altitude of 6900 ft. and a velocity of 480 ft/sec. It is based on the ideas of Refs. (1) and (2).

The guidance routine consists of six modes: Acquisition, Energy Dissipation, Turn-in, Initial Approach, Heading Alignment, and Final Approach. The horizontal geometry is illustrated in Figure 1 in which the circled numbers refer to the various modes. The Acquisition Mode begins at 100,000 ft altitude, contains an angle-of-attack transition maneuver, and ends when the vehicle is within about 15 n. mi. of the runway. Energy dissipation involves flight in the vicinity of the runway around a cylinder of radius 13.5 n. mi. During this mode the vehicle descends from about 50,000 ft altitude to 26,000 ft. This helical flight usually comprises less than one half of a revolution around the cylinder. The next three modes, i. e. Turn-in, Initial Approach, and Heading Alignment, constitute a two-turn maneuver to place the vehicle on the appropriate final approach path. The Final Approach Mode establishes the proper interfaces with the Terminal Guidance Routine for the final maneuvers required to land on the runway.

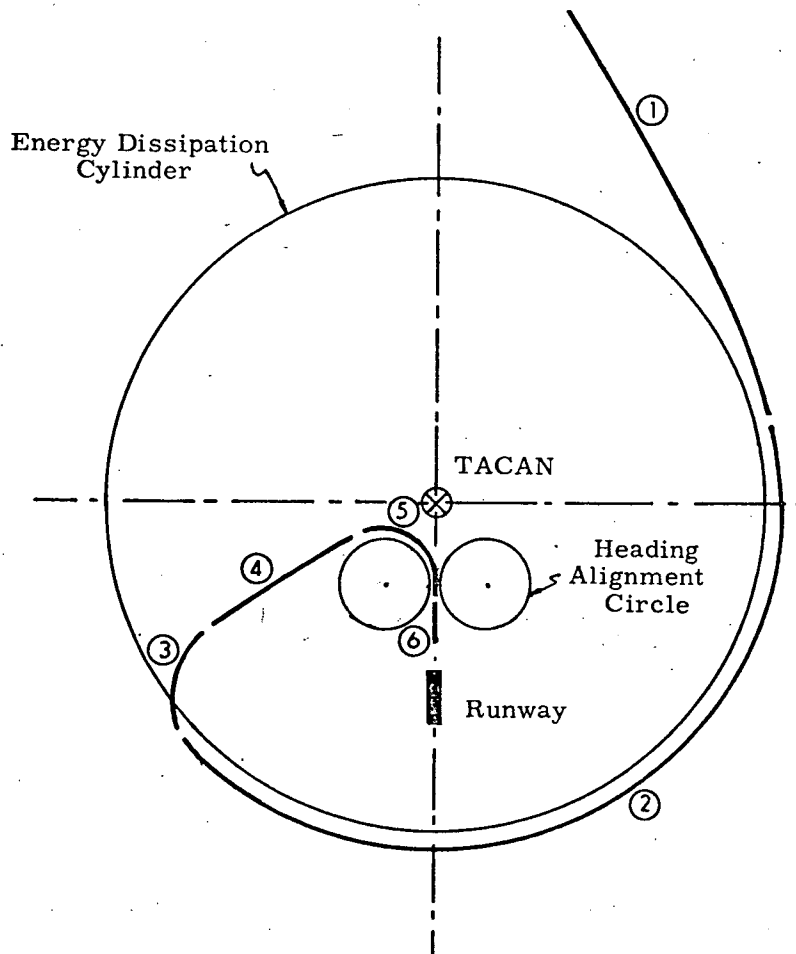


Figure 1. Horizontal Geometry, Approach Guidance

2. FUNCTIONAL FLOW DIAGRAM

The basic flow of the Approach Guidance Routine is shown in Figure 2.

After the routine is entered and initialized, targeting computations are made to obtain the current values of position and velocity, and direction parameters of the vehicle relative to the desired touchdown point. Next, the mode is selected based on the current trajectory conditions, and quantities unique to the specific mode are computed.

The angle-of-attack command is used for vertical control and is computed during the first part of Mode 1 so as to accomplish a constant (-0.3 deg/sec) angle-of-attack transition maneuver. During the remainder of Mode 1 and for Modes 2 and 3, an angle-of-attack which will yield a constant ($210 \frac{\text{lb}}{\text{ft}^2}$) dynamic pressure is commanded. Finally, during the last three modes, the angle-of-attack which will cause the vehicle to fly at a constant flight path angle (-11 deg) is commanded.

The roll-angle command is used for horizontal control and is computed for the various modes as shown in the following table.

Table 1
Geometric Criteria for Roll-Angle Command

<u>Mode</u>	<u>Geometric Criterion</u>
1	Tangent to Energy Dissipation Cylinder (EDC)
2	Fly on EDC
3	Turn toward center of EDC
4	Tangent to Heading Alignment Cylinder (HAC)
5	Fly on HAC
6	Align into vertical runway plane

Finally, the rudder flare or speed brake is deployed during the last three modes in order to achieve a speed of 480 f/s at the end of approach guidance.

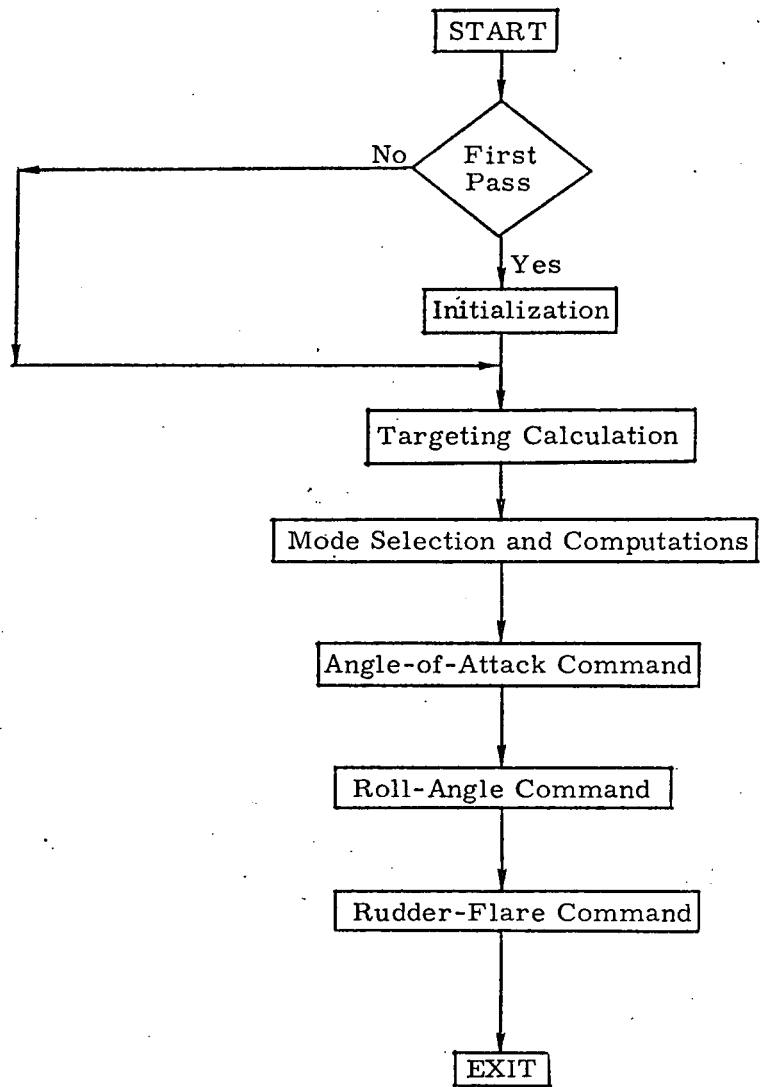


Figure 2. Functional Flow Diagram, Approach Guidance

3. INPUT AND OUTPUT VARIABLES

Input Variables

$\underline{\rho}_R$	Vehicle position vector (RW Coord.)
\underline{v}_R	Vehicle velocity vector (RW Coordinate)
\underline{a}	Vehicle acceleration vector (RW Coord.)
ψ_{RW}	Runway azimuth (0 - 360 ^o)
Δt	Time interval between guidance updates

Output Variables

ϕ_c	Command roll angle
α_c	Command angle-of-attack
d_c	Command rudder flare

4. DESCRIPTION OF EQUATIONS

The guidance system task can be separated into three parts; (1) lateral guidance (2) vertical guidance, and (3) speed control. Lateral guidance is accomplished by commanding vehicle roll angle, vertical guidance is accomplished by commanding angle of attack, and speed control is attained by deploying the speed brake.

4.1 Lateral Guidance

Figure 3 illustrates the essential geometry of the lateral guidance problem.

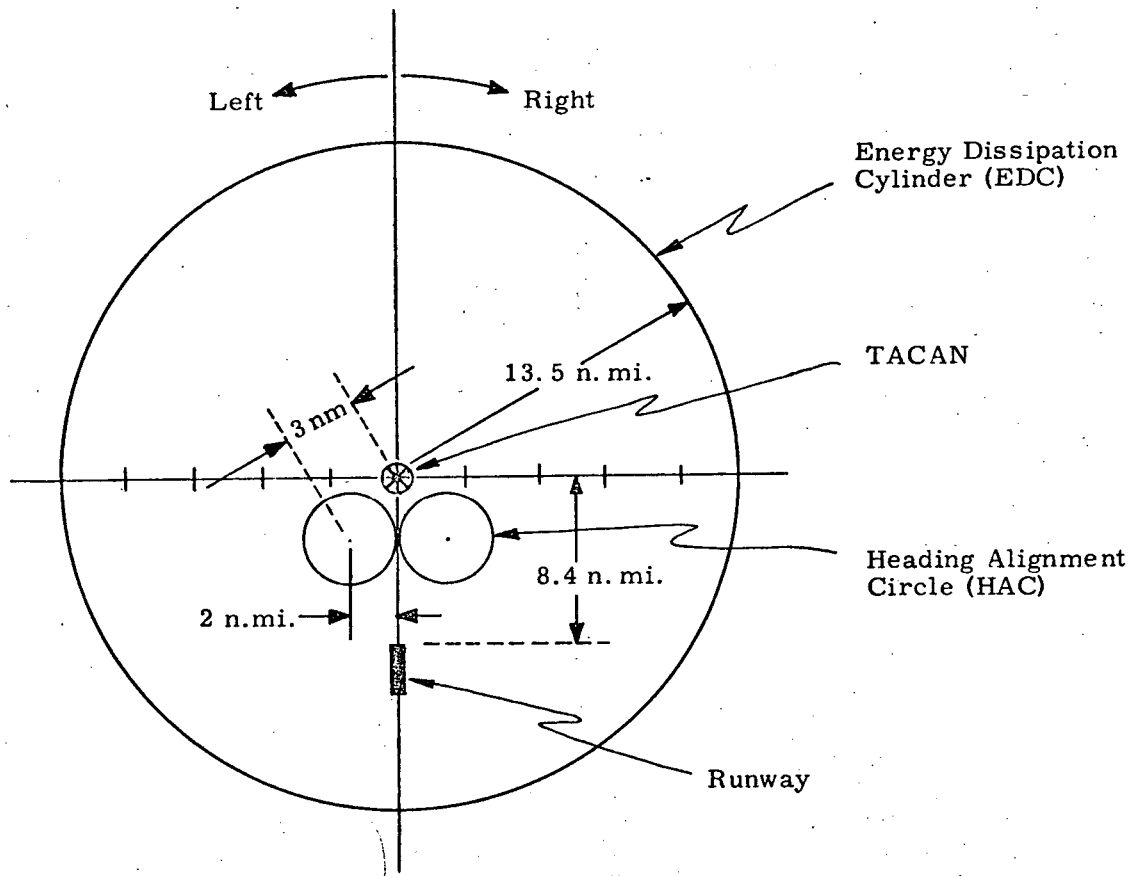


Figure 1. Lateral Guidance Geometry

Figure 3. Lateral Guidance Geometry

The guidance task begins with the vehicle about 35 n. mi. from the TACAN (ED center) at an altitude of 100,000 ft and velocity of 2000 fps. The guidance system is initially in the Acquisition Mode, which commands heading so the vehicle follows a path tangent to the energy dissipation cylinder (EDC). From any point outside the cylinder there are two such tangent paths and the guidance system chooses the tangent nearest to the initial heading of the vehicle. When the vehicle is within 15 n. mi. of the TACAN the guidance mode changes to Energy Dissipation. This mode commands heading so the vehicle maintains the circular path necessary to stay on the EDC. Typically, the vehicle enters the EDC at about 50,000 ft altitude and leaves the EDC at 26,000 ft after travelling about half way round the cylinder. Both potential energy, in the form of altitude, and kinetic energy, in the form of velocity, are dissipated on the EDC. When the vehicle reaches 26,000 ft, the Turn-in mode takes command. This mode simply commands heading toward the TACAN. When the vehicle comes within 11 n. mi. of the TACAN, command switches to the Initial Approach mode. This mode commands heading so the vehicle flies a path tangent to the nearest heading alignment circle (HAC). If the vehicle is in the right half cylinder, then it guides toward the right (HAC), and on the left it guides to the left (HAC). When the vehicle reaches 2.15 n. mi. from the center of the appropriate HAC, the mode switches to Heading Alignment, which commands a 2 n. mi. radius circle to the runway heading. The Final Approach Mode commands vehicle aligned with runway. Command is then given over to the terminal guidance system.

Lateral guidance is accomplished by rolling the vehicle to attain desired headings in the various modes, as described above. The roll command is

$$\Phi = \frac{\Delta \psi_c \cdot v}{12g}$$

where Φ = commanded roll angle (deg)
 $\Delta \psi_c$ = angle between actual heading and desired heading (deg)
 v = velocity (fps) w. r. t. air mass
 g = 32.2 ft/sec².

This control is used in all modes except Energy Dissipation when integral control is added to eliminate steady state errors. In the ED Mode $\Delta\psi_c$ is replaced by $\Delta\psi'_c$ where

$$\Delta\psi'_c = \Delta\psi_c + .2 \int_{t_0}^t \Delta\psi_c dt$$

t_0 = beginning of ED mode.

4.2 Vertical Guidance

During each of the guidance modes described above, the vertical path of the vehicle must be carefully controlled. The dominant vehicle dynamic mode, affecting altitude, is the long period or phugoid mode. In a relatively low drag vehicle such as the shuttle, the phugoid mode is lightly damped and its frequency of oscillation can be determined approximately as $\omega_n = 2 \frac{g}{V}$.

Transition Maneuver. - Approach Guidance begins at a velocity of about Mach 2. At this time the angle-of-attack has to be reduced gradually, in order to bring the vehicle into the region in which it operates on the front side of the L/D curve.

The angle of attack command is:

$$\alpha_c = \alpha - \Delta\alpha$$

where

α_c - angle-of-attack command

α - current angle-of-attack

$\Delta\alpha$ - change (about 0.3 deg/sec)

This phase is ended when once α is less than 10 degrees.

Constant Dynamic Pressure. - During the Acquisition, Energy Dissipation and Turn-in Modes, the vehicle is guided along a constant dynamic pressure path. Vertical specific force is commanded, based on dynamic pressure and dynamic-pressure rate feedback as follows:

$$l_D = -k_1(q - q_D) - k_2(\dot{q}) + g$$

where

l_D - desired vertical specific force

q - dynamic pressure

q_D - pre-selected desired dynamic pressure

\dot{q} - $d(q)/dt$

g - gravity

k_1, k_2 - control gains

Constant Flight Path Angle. - During, the Initial Approach, HA Turn, and Final Approach Modes, the vehicle follows a linear altitude vs. range-to-go trajectory

$$h_R = c_1 + \frac{(h_1 - c_2)}{\rho_{P1}} \rho_P$$

where

h_R - desired altitude

ρ_P - range-to-go from now to key point

ρ_{P1} - range to go at beginning of Initial Approach

h_1 - altitude at beginning of Initial Approach

c_1, c_2 - constants

The vertical specific force is commanded based on altitude and altitude-rate feedback

$$l_D = -k_1(h - h_R) - k_2(\dot{h} - \dot{h}_R) + g$$

where

\dot{h} - altitude rate

\dot{h}_R - desired altitude rate

(c) Speed Control

In order to attain appropriate velocity at the end of the final approach and to control dynamic pressure, the vehicle speed brake is applied during and after the Initial Approach Mode. The control logic is as follows:

$$\text{Rudder flare angle} \left\{ \begin{array}{l} = 0^{\circ} \quad v < 480 \text{ fps} \\ = 2 (v - 480^{\circ}), \quad 480 < v < 510 \text{ fps} \\ = 60^{\circ} \quad v > 510 \text{ fps} \end{array} \right.$$

5. DETAILED FLOW DIAGRAMS

This section contains detailed flow diagrams of the Approach Guidance Routine.

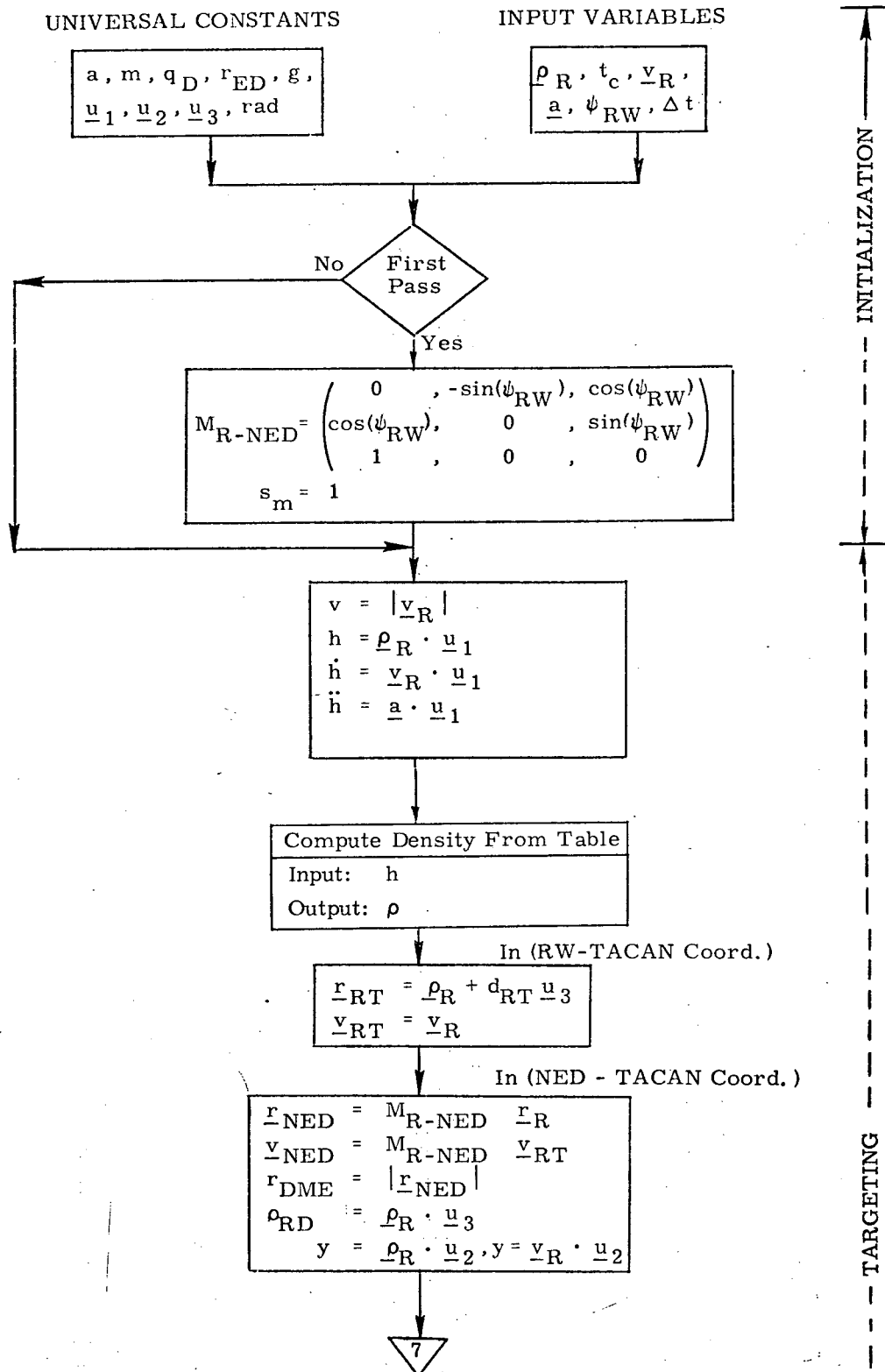


Figure 4a. Detailed Flow Diagram, Approach Guidance Routine

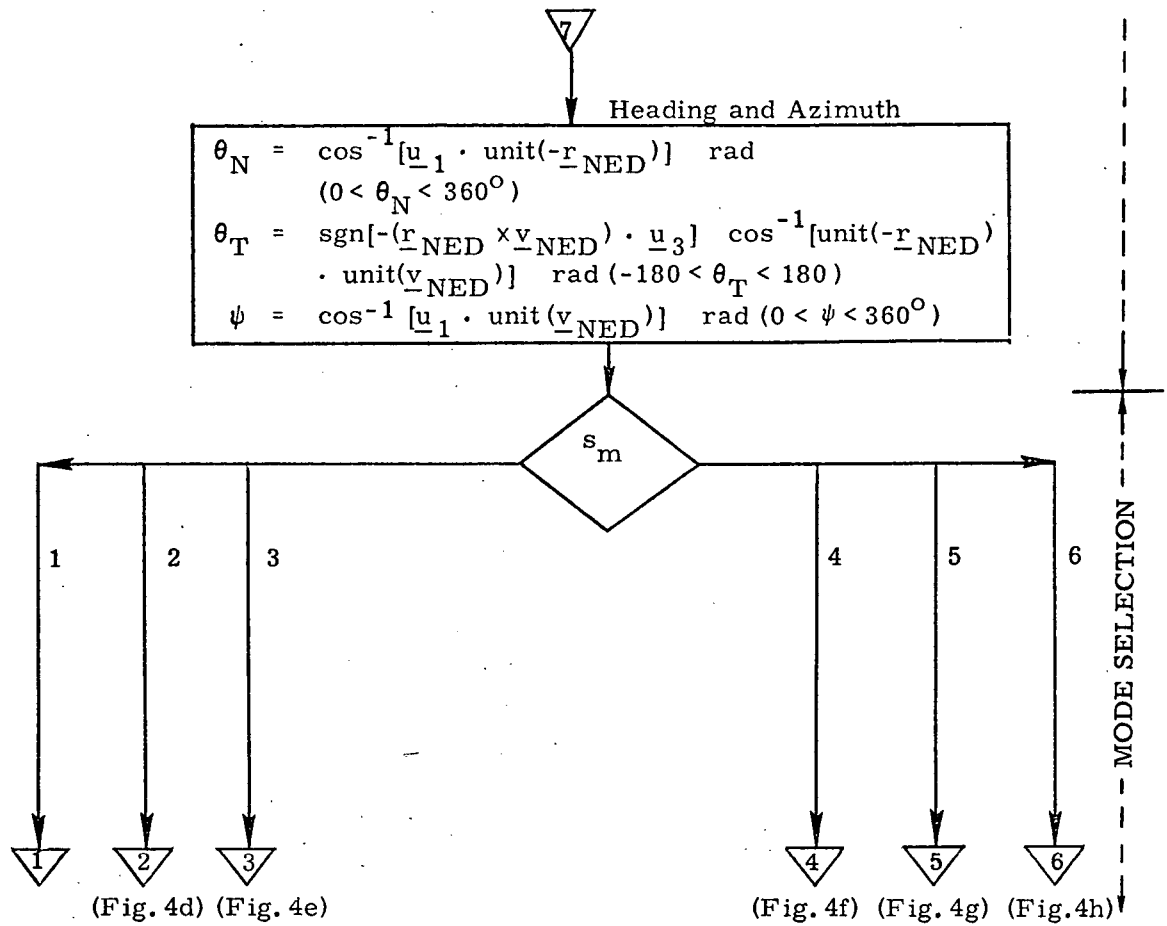
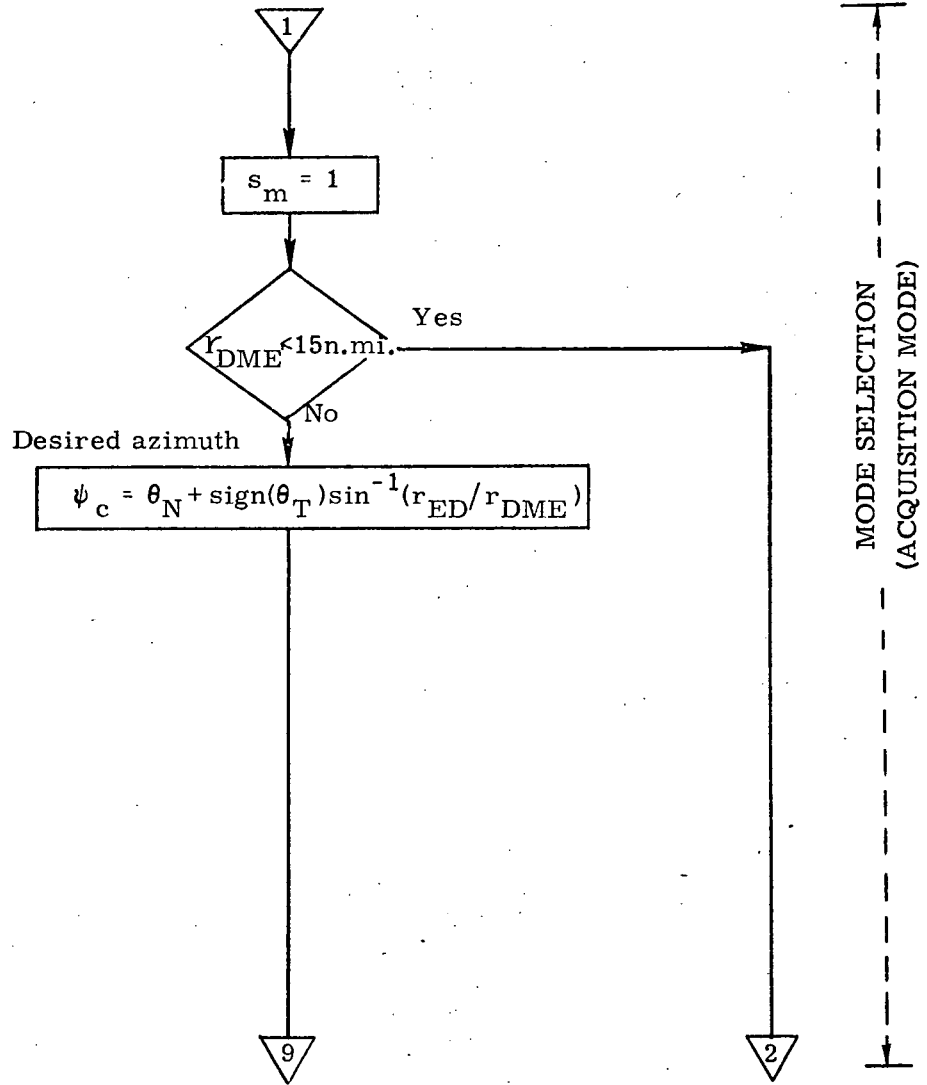
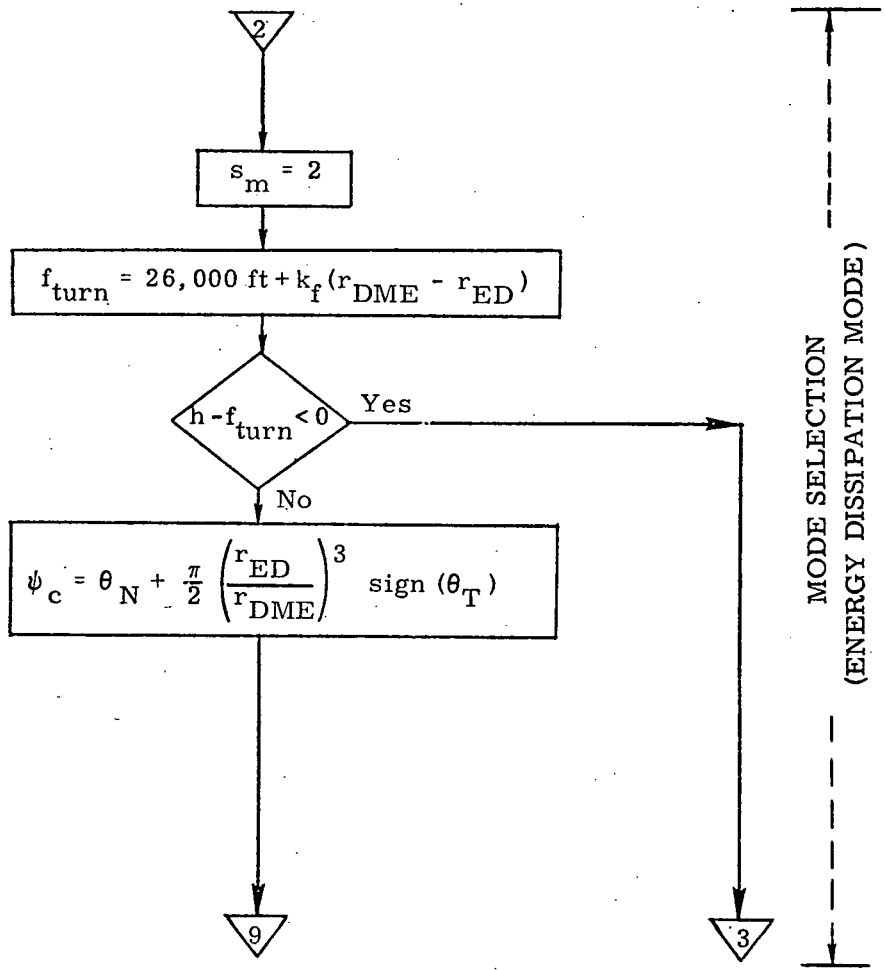


Figure 4b. Detailed Flow Diagram, Approach Guidance Routine



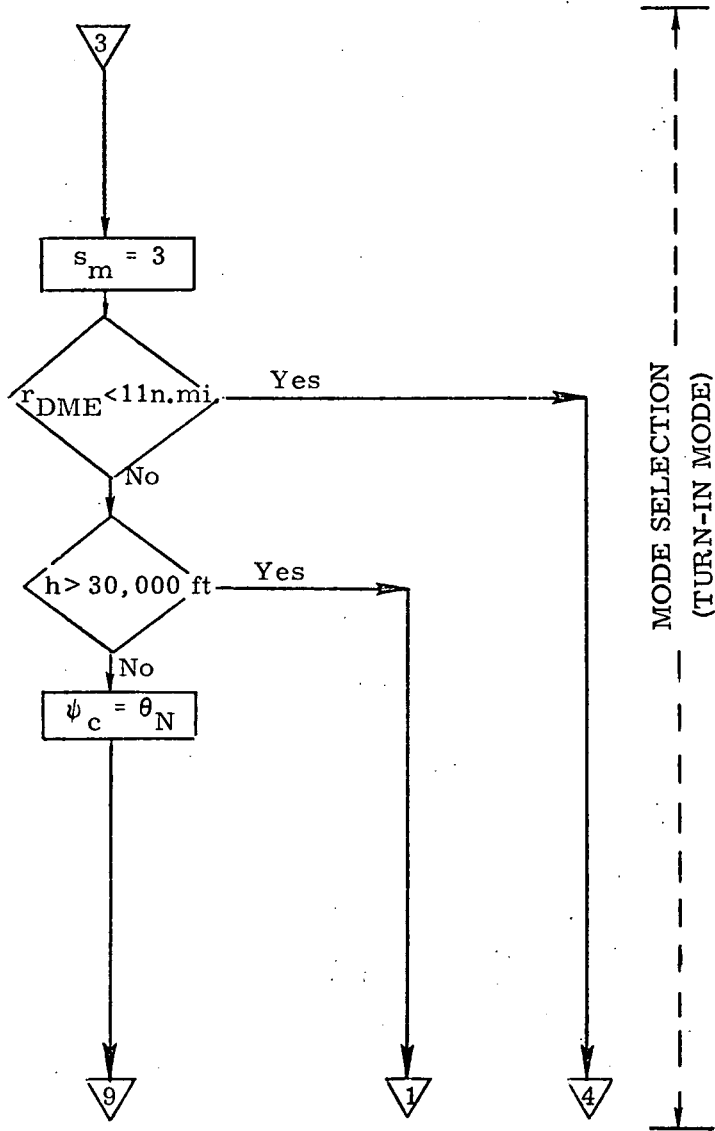
(Figure 4i)

Figure 4c. Detailed Flow Diagram, Approach Guidance Routine



(Figure 4i)

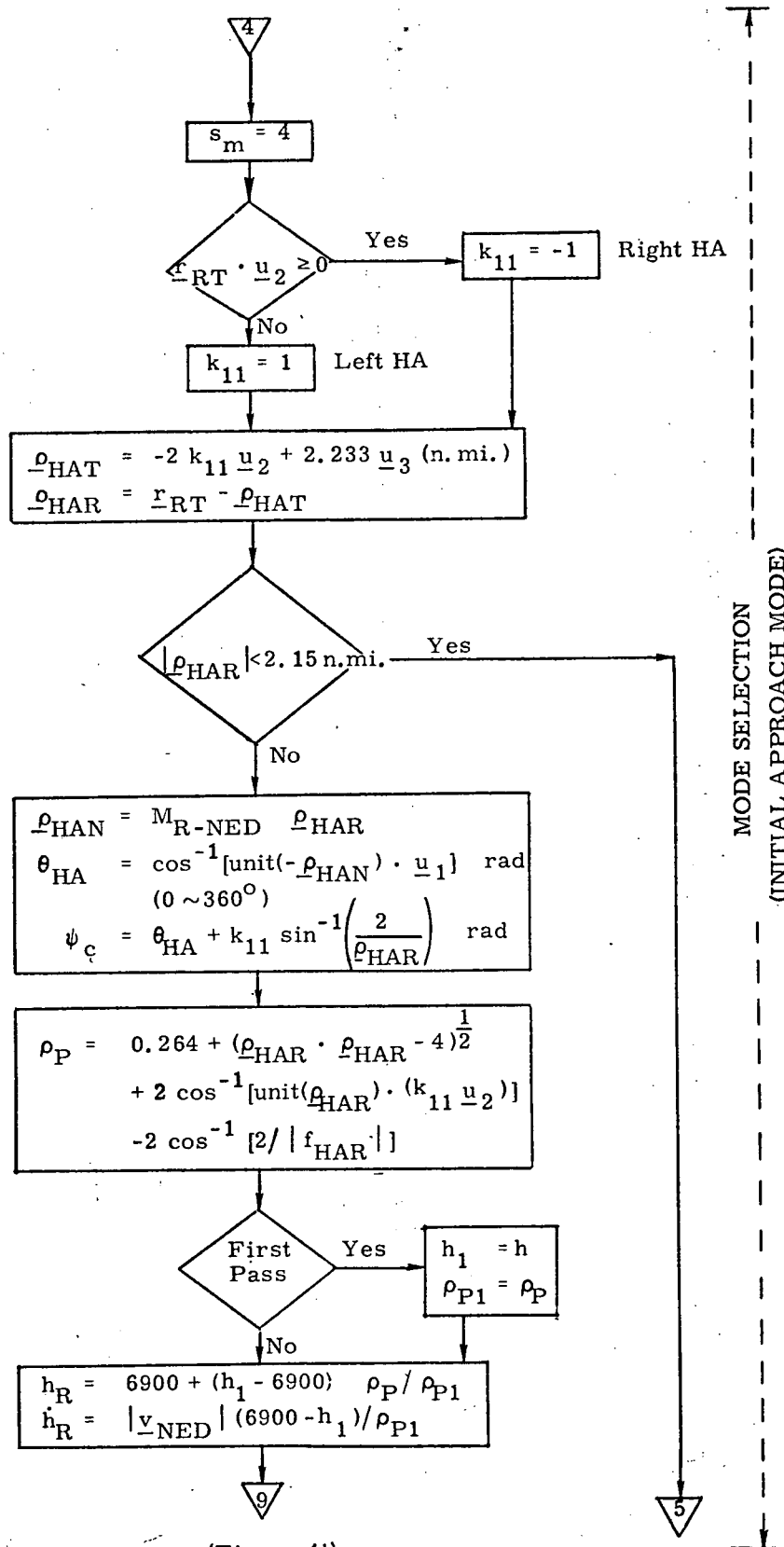
Figure 4d. Detailed Flow Diagram, Approach Guidance Routine



(Figure 4i)

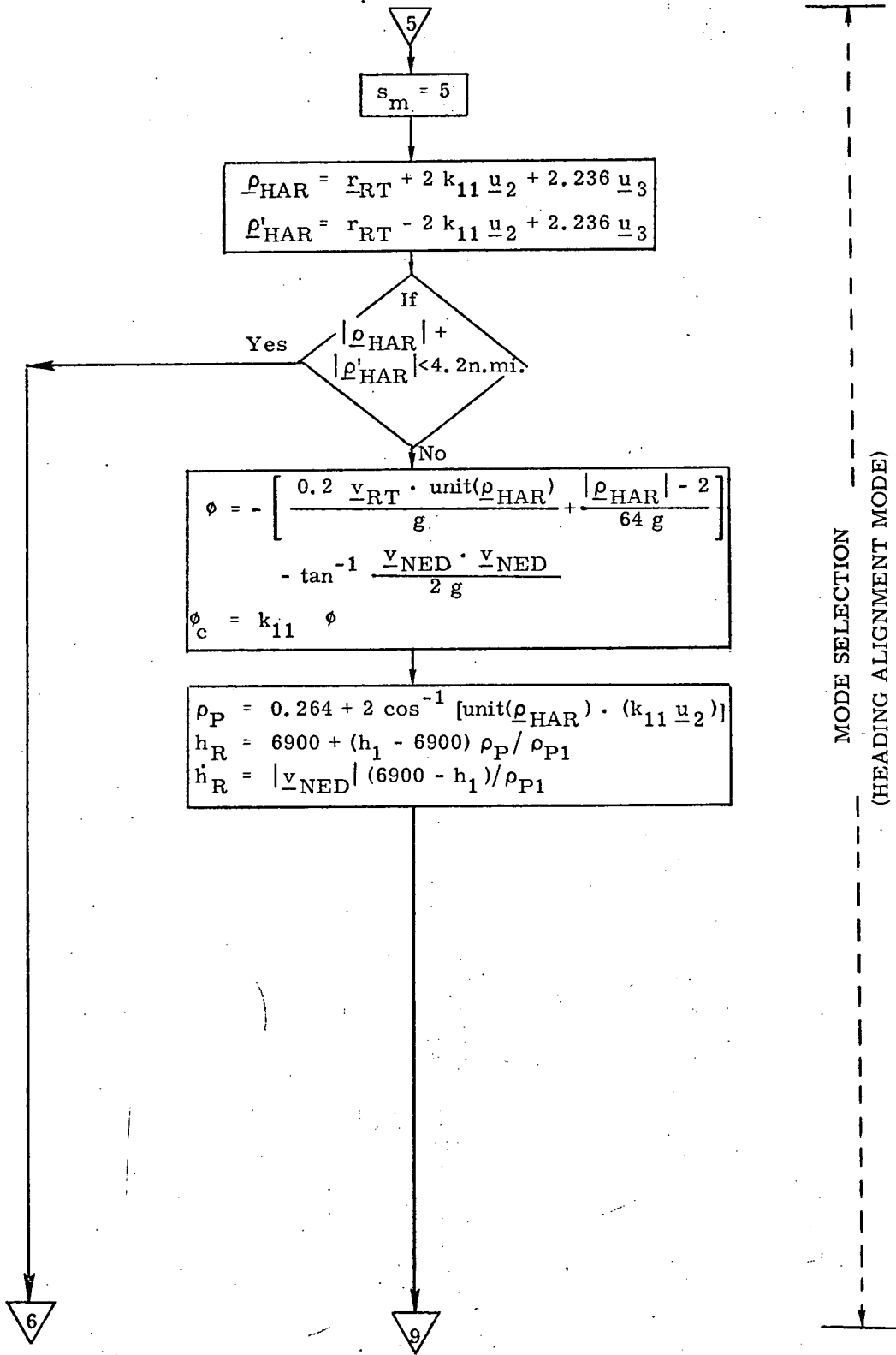
(Figure 4c)

Figure 4e. Detailed Flow Diagram, Approach Guidance Routine



(Figure 4i)

Figure 4f. Detailed Flow Diagram, Approach Guidance Routine



(Figure 4i)

Figure 4g. Detailed Flow Diagram, Approach Guidance Routine

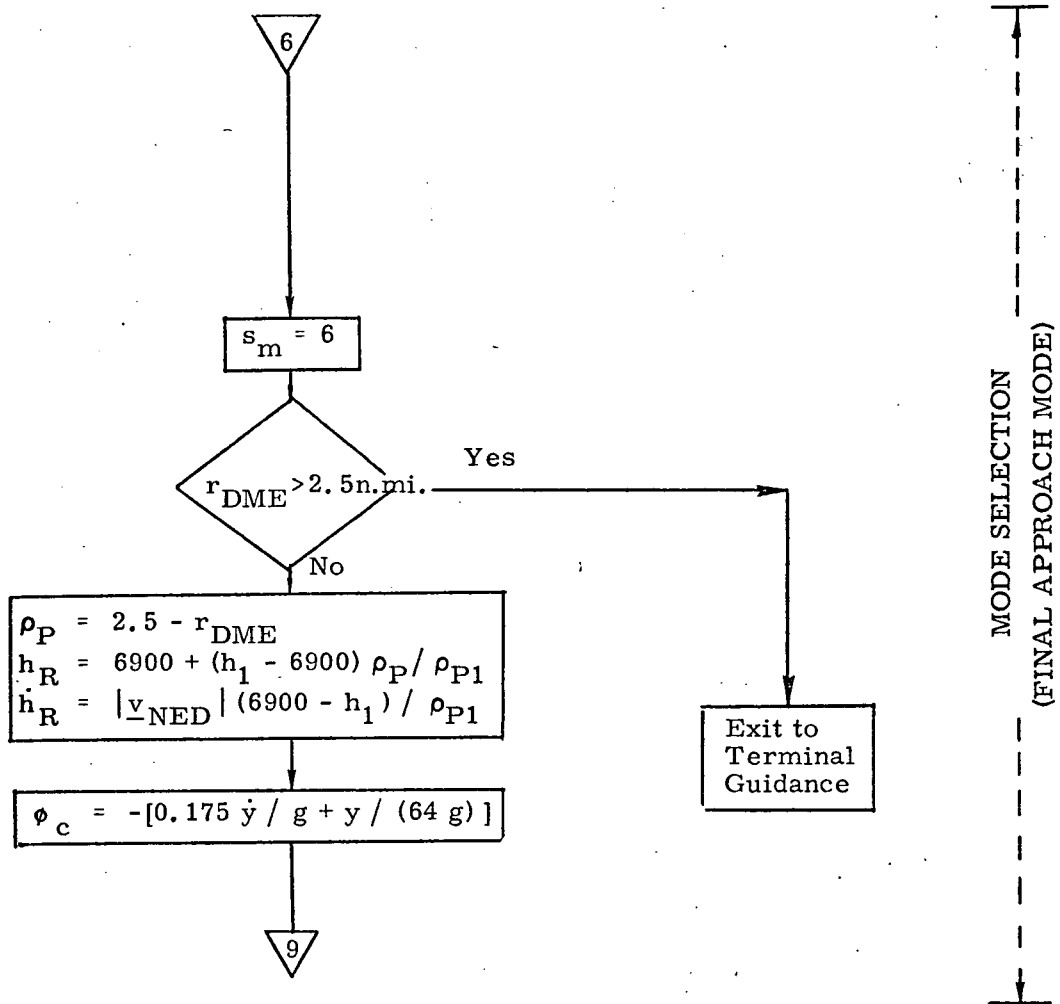


Figure 4h. Detailed Flow Diagram, Approach Guidance Routine

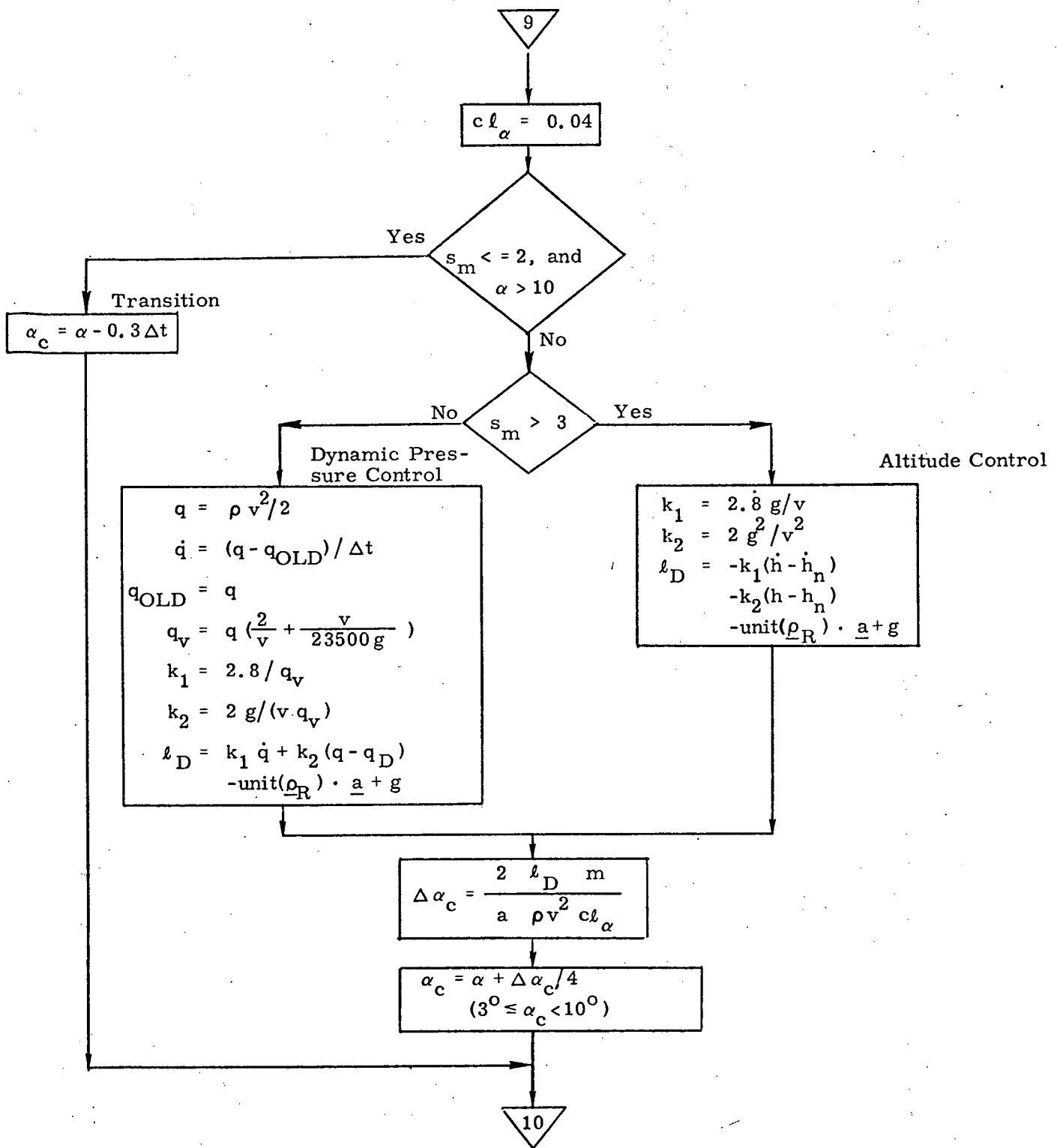


Figure 4i. Detailed Flow Diagram, Approach Guidance Routine

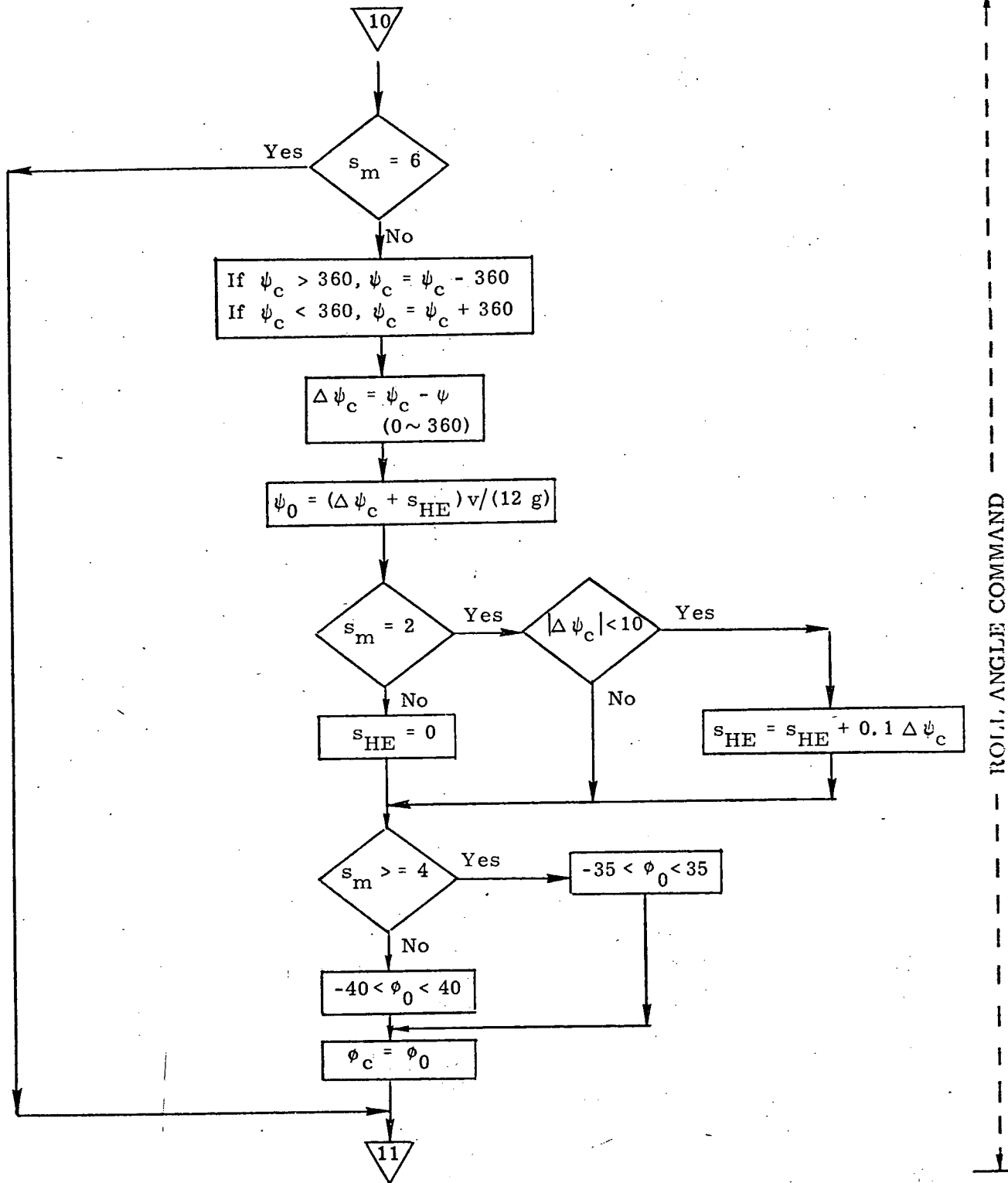


Figure 4j. Detailed Flow Diagram, Approach Guidance Routine

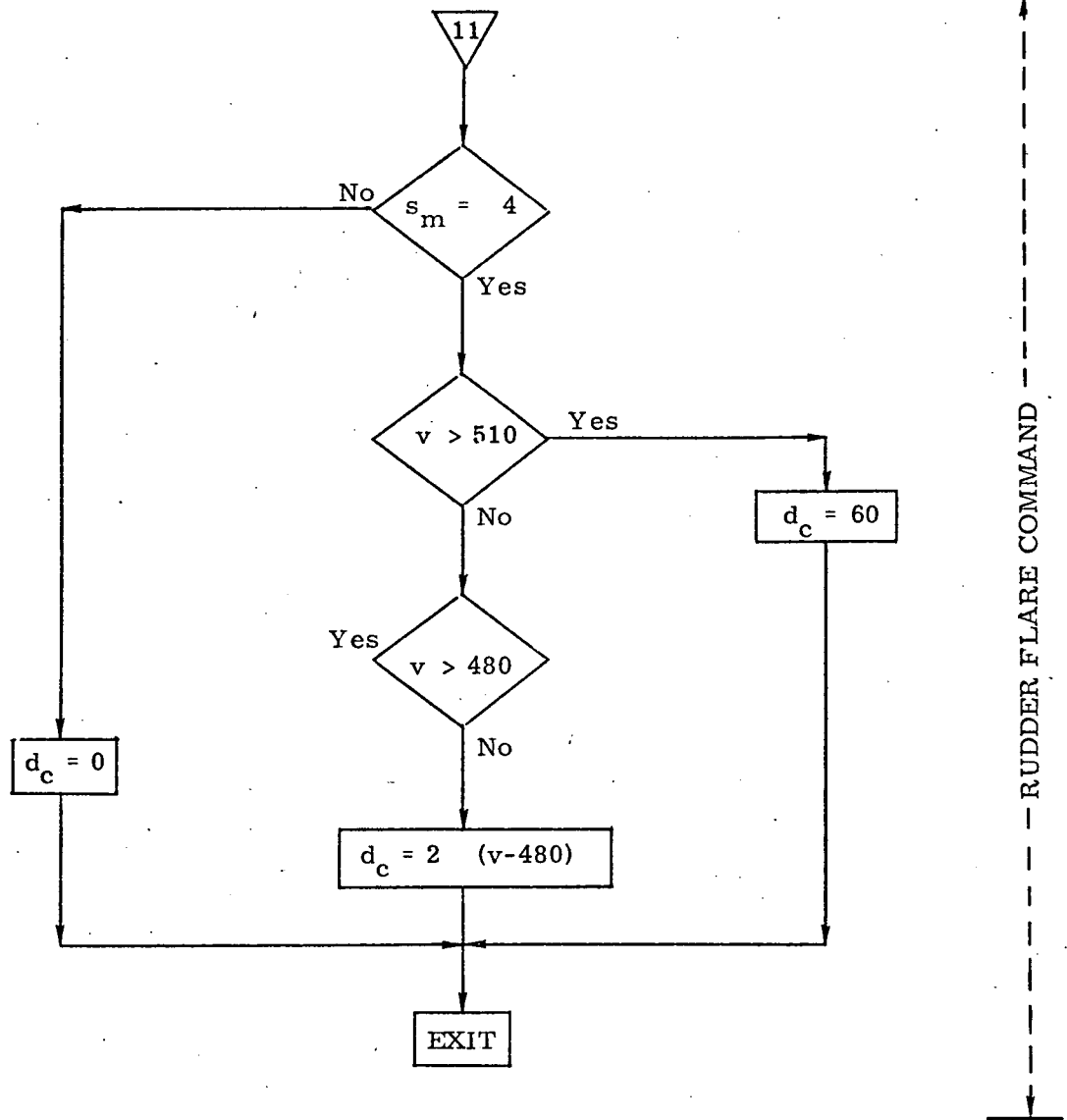


Figure 4k. Detailed Flow Diagram, Approach Guidance Routine

REFERENCES

1. Deyst, J., Tao, M., "Approach Phase Guidance System", MIT Draper Lab, 23A STS Memo No. 11-A, September 1972.
2. Eterno, J., "Terminal Area Guidance for the Delta-Wing Orbiter", CG43-71M-89.

Do not Reproduce

23A SHUTTLE DISTRIBUTION LIST

INTERNAL (82)		EXTERNAL (34)	
<u>23A</u>	(35)	<u>EA2</u>	(1)
<u>23B</u>	(2)	W. Bradford	
M. Hamilton		<u>EG</u>	(1)
J. Kernan		D. Cheatham	
<u>23C</u>	(22)	<u>EG2</u>	(12)
<u>23D</u>	(1)	K. Cox	
I. Johnson		D. Dyer	
<u>23I</u>	(2)	E. Kubiak	
R. McKern		F. Elam	
W. Tanner		B. Marcantel	
<u>23N</u>	(1)	W. Peters	
G. Ogletree		C. Price	
<u>23P</u>	(13)	R. Saldana	
R. Battin		E. Smith	
S. Copps		J. Suddath	
D. Dolan (4)		J. Sunkel	
T. Edelbaum		G. Zacharias	
D. Hoag		<u>EG3</u>	(1)
L. Larson		J. Lawrence	
R. Larson		<u>EG4</u>	(1)
R. Millard		P. Sollock	
R. Ragan		<u>EG5</u>	(1)
N. Sears		C. Manry	
<u>23S</u>	(3)	<u>EG6</u>	(1)
G. Edmonds		R. Reid	
P. Felleman		<u>EG7</u>	(2)
R. White		C. Hackler	
<u>33</u>	(2)	J. Hanaway	
L. Drane		<u>EG/MIT</u>	(3)
H. Laning		A. Cook	
<u>35</u>	(1)	E. Olsson	
M. Johnston		G. Silver	
		<u>FA</u>	(1)
		H. Tindall	
		<u>FD7</u>	(1)
		A. Hambleton	
		<u>FM4</u>	(3)
		B. Cockrell	
		P. Pixley	
		R. Savely	
		<u>FM6</u>	(2)
		R. Becker	
		P. Shannahan	
		<u>FM7</u>	(2)
		S. Mann	
		R. Nobles	
		<u>FS6</u>	(1)
		J. Garman	
		<u>FM</u>	(1)
		T. Gibson	

Additional for GN&C Equation Documents (21)

G. Levine (10), E. Olsson (5), J. Rogers BC7, E. Smith (5)